We thank the Referee for the insightful comments. We have revised our manuscript according to the suggestions of the Referee's comments and our responses to the comments are as follows. The Referee's comments are in black, authors' responses are in blue, and changes to the manuscript are in red color text.

This study investigates the formation of secondary organic aerosols from the photooxidation of furan at different NOx and RH levels. SOA yields were measured using NaCl seeds to provide surface area for the partitioning of SOA-forming vapors. The chemical composition, in particular organic functional groups and a selection of molecular products, was characterized by FTIR and ESI-MS. The authors found a strong dependence of the measured SOA concentration, mass yield, and the intensity of individual functionalities on the initial VOC/NOx ratios and RH levels in a series of experiments conducted, and suggested that NOx and RH play an important role in the SOA formation from furan oxidation by altering the chemical pathways, e.g., aqueous phase chemistry, that essentially lead to SOA. This conclusion, however, is heavily drawn from the inadequate data analysis and interpretation, and lacks fundamental understanding of the predominant chemistry that occurs in the chamber experiments performed.

<u>NOx dependence of SOA yields</u>

In this study, photolysis of NO2 was used to generate O3, which further undergoes photolysis and reaction with H2O to generate OH radicals. The initial VOC/NOx ratio in the performed experiments ranges from ~7 to ~48. With the presence of hundreds of ppb levels of furan at the beginning of the experiment, furan is not completely oxidized at the end and the measured SOA mass is mostly composed of the very first few generations of oxidation products. As the initial VOC/NOx ratio decreases, more NO2 will be available for the formation of O3 and consequently OH radicals. **The observed 'NOx-effect' here is essentially the OH effect: higher OH levels result in more furan consumed, thus producing more SOA mass and higher SOA yield.**

This OH effect on SOA production has been well studied and understood in the community.

Author reply:

In our experiments, the OH radical was indeed produced during the photooxidation of furan instead of being added before the experiments started. But the original intension of our study was not to determine the OH effect on furan SOA formation. As indicated previously, SOA yields increase with increasing NOx concentration at low NOx levels and then decrease at higher NOx concentration (Sarrafzadeh et al., 2016a; Loza et al., 2014; Hoyle et al., 2011; Chan et al., 2010). All these studies demonstrated that the increase of SOA yield at low NOx levels was attributed to an increase of OH concentration. After eliminating the effect of OH concentration on the SOA mass growth, the SOA yield only decreased with increasing NOx concentration.

To control the effect of OH concentration on furan SOA formation in the present work, four more experiments have been added with additional injection of H_2O_2 as OH precursor before the experiments started. The results suggested that there remains a positive correlation between SOA formation and NOx concentration as shown in Table S1 and Fig. 3. To further understand the effect of NOx level on SOA formation, four more experiments were carried out for HESI-Q Exactive-Orbitrap MS detection. The MS results revealed the formation of a number of cyclical hydroxyl nitrates and dihydroxyl dinitrates with low-volatility, which can significantly contribute to the SOA formation (Schwantes et al., 2019). To provide a better illustration of the NOx effect on SOA formation, the following changes have been made to the revised manuscript.

Page 7, line 2:

"To further assess the effect of OH produced during the furan-NOx photooxidation, four experiments (Table S1, Exp.13-16) were conducted by injecting H_2O_2 in the chamber before the experiments started. For Exp.6-12, different RH levels coupled

with similar furan/NOx ratios were monitored to assess the RH impact on SOA formation. To analyze the SOA composition, five additional experiments (Table S2, Exp. 17-21) were carried out to analyze the HESI-Q Exactive-Orbitrap MS, which intended to compare the role of NOx and RH on the SOA formation."

Page 9, line 5:

"It is generally accepted that experiments with low NOx levels lead to higher SOA yields than those with higher NOx levels at the same VOC concentration (Song et al., 2005). However, as shown in Fig. 3, an increasing SOA mass concentration and SOA yield with increasing NOx was observed. There are two possible explanations to this phenomenon: (i) The concentration of OH radicals produced *in situ* in the present study before additional source of OH was insufficient to produce a considerable amount of SOA under low-NOx conditions. As shown in Fig. S3, the OH concentration exhibits a gradual increase with NOx concentration and there appears to be a correlation between NOx concentration, OH concentration and SOA yield. Therefore, at low-NOx conditions, the increase of SOA yield was attributed to an increase of OH concentration, which was affected by OH recycling following reaction (R6) (see Fig. 1) and contributed to the enhancement of SOA formation. This result is consistent with a previous study concerning the impact of NOx and OH on SOA formation from β-pinene photooxidation, which has proved that the positive correlation between SOA yield and NOx levels ($[VOC]_0/[NOx]_0 > 10$ ppbC/ppb) was caused by the NOx–induced increase of OH concentration (Sarrafzadeh et al., 2016b). (ii) Differently, Sarrafzadeh et al. found that after eliminating the effect of OH concentration on SOA mass growth, SOA yield only decreased with increasing NOx levels (Sarrafzadeh et al., 2016b). To further investigate the NOx effect on furan generated SOA formation under adequate OH conditions, four more experiments (see Table S1) were carried out with additional injection of H_2O_2 as the OH radical source before the start of each experiment. The SOA yield trend at different C_4H_4O/NOx ratios is also shown in Fig. 3. The continuous growth trend of SOA yield with increasing NOx concentration at a relative high NOx level may result from the

partitioning of generated semi/low-volatility compounds (multifunctional nitrates and dinitrates) into the particle phase, leading to significant furan SOA formation under high NOx conditions. Similarly, SOA from OH-initiated isoprene oxidation under high-NOx conditions was comprehensively investigated by Schwantes et al., who suggested that low volatility hydroxyl nitrates and dihydroxyl dinitrates generated conspicuously more aerosol than previously thought (Schwantes et al., 2019). Our results showing the increase of SOA mass formation at high-NOx conditions also agree with a previous study, which indicated that a high level of NO_2 can participate in the OH-induced reaction of guaiacol, consequently leading to the formation of organic nitrates and the enhancement of guaiacol SOA formation (Liu et al., 2019a). ”

Page 11, line 21:

“The MS spectra of generated species from different NOx level and RH conditions, which show evidence for the OH-furan reaction, are presented in Fig. 7 and Fig. 8, respectively. The major peaks are m/z^+ 85.0018, 101.0894, and 185.0504 in the positive ion mode, and m/z^- 146.0161, 225.0125 and 263.0132 in the negative ion mode. The prominent peaks in the HR-MS spectra detected on negative ion mode are comprised of various functionalized hydroxyl nitrates and dihydroxyl dinitrates. However, in the positive ion mode analysis, most carbonyl components were detected. The assignments of these ion peaks, the molecular weights of the products observed, and proposed structures are summarized in Table 3. These detected compounds provide additional evidence for the proposed radical reaction mechanism.”

Page 12, line 4:

“(i) decompose and then react with O_2 to yield a 1,4-aldoester (A), (ii) react with $NO_2/NO/O_2$ to form hydroxyl nitrate compound isomers with m/z^- 146., or (iii) react with O_2 to form unsaturated products and hydroxyfuranone (B) and 1,4-aldoacid (C). The ring-opened alkylperoxy radical generated from (d) can decompose to generate an unsaturated 1,4-dialdehyde (D). The formation of 1,4-dialdehyde with m/z^+ 85 detected in the positive ion mode suggests that these unsaturated 1,4-dicarbonyls are

formed after initial OH addition at 2- or 5-positions. We note that OH radical addition at 2, 3-positions would lead to carbonyl product isomers with same m/z^+ 101. In addition, some dihydroxyl dinitrates with m/z^- 225 were also detected in negative ion mode. However, the pathways favouring the generation of these dihydroxyl dinitrates could only take place under high NOx levels. Scheme 1 shows the formation of second-generation products hemiacetals (E) via the reactions of the hydroxyfuranone (B) with 1,4-dialdehyde (D). After uptake from the gas-phase, the combination of hydroxyfuranone with 4-dialdehyde appeared to occur by H-abstraction, followed by dehydration, thus forming m/z^+ 185 compounds. This reaction pathway has also been identified in previous studies of OH-initiated reactions of furans (Strollo and Ziemann, 2013; Aschmann et al., 2014). According to the results of HR-MS, this aqueous phase reaction is more favoured in aqueous particles."

Page 13, line 4:

"However, in the present study, an increasing trend of SOA formation was observed with the increase of NOx concentration. As shown in the HESI-Q Exactive Orbitrap-MS results, all the detected primary products are carbonyl-rich, and even the organonitrates have at least two carbonyl functional groups. These carbonyl-containing products have lower volatility and contribute to the SOA formation. The peak intensities in the MS of the products (m/z^+ 85, 101) generated by the pathways involving HO_2 (as indicated by the scheme 1) decreased with the increase of NOx concentration. Additionally, more products of dihydroxyl dinitrates (m/z^- 225) with multifunctional groups were detected under high NOx conditions. As shown in Scheme 1, the multifunctional organonitrates detected in negative ion mode are produced mostly from later-generation chemistry. Hydroxyl nitrates with m/z^- 149 can be formed through pathways 1-a, 2-a, and 3-a by the reaction of RO_2 with NOx. We note that the m/z^- 149 compound was detected both at low NOx levels and high NOx levels. However, the peak intensity of this product was decreased with increasing NOx concentration. This phenomenon might be caused by the later-reaction of the unsaturated hydroxyl nitrates going through a second

OH-initiated reaction and leading to the formation of the dihydroxyl dinitrate with m/z^- 225. In addition, the peak intensities changes of SOA products detected in the positive mode, such as, the peaks at m/z^+ 85 and 101 were reduced under high NOx conditions, which resulted from the fact that the RO_2 radical fate was dominated by the pathway of RO_2+NO or RO_2+NO_2. This result supports that the fate of RO_2 is not a single channel reaction. There exists a competition between RO_2 reacting with NOx and with HO_2 under high NOx conditions but the former pathway is more favourable. There are two pathways for hydroxyl nitrates formation from RO_2 radicals in the presence of NOx according to which RO_2 radicals may react with NO and NO_2 to form $RONO_2$ and $ROONO_2$, respectively (Kroll and Seinfeld, 2008). However, the formed peroxynitrates could easily thermally dissociate and convert to $RONO_2$.

Furthermore, by analyzing the OH concentration and products components, we conclude that there are two possible explanations for the increasing trend of SOA yield as the NOx level increases: (i) the SOA production is closely related to the oxidation capacity in the photooxidation experiments. Experiments conducted under different NOx levels indicate that the OH concentration is controlled by the NOx level if there is no additional OH precursor added before the start of the experiment. As shown in Fig. S3, an increase in NOx level results in more OH generation and a faster furan decay rate. This justifies the observed higher SOA mass concentration and higher SOA yield. (ii) HRMS fragments associated with multifunctional organonitrates are enhanced under high NOx conditions (Fig. 7). As presented in Scheme 1, the furan dihydroxyl dinitrates are generated from the first-generation hydroxyl nitrate reacting with OH to form a peroxy radical, which reacts thereafter with NO. Together with multifunctional hydroxyl nitrates, these low-volatility species can easily partition into the particle phase and increase the SOA mass concentration. More importantly, the seed particle added initially plays an important role in the processes of gas-particle partitioning as indicated by a recent study, which showed that sufficient seed surface area at the start of the reaction largely suppressed the effects of vapour wall losses of low-volatility compounds (Schwantes et al., 2019).

Therefore, the NaCl seed particle added in the present work promoted the partitioning of the formed low-volatility functional organonitrates."

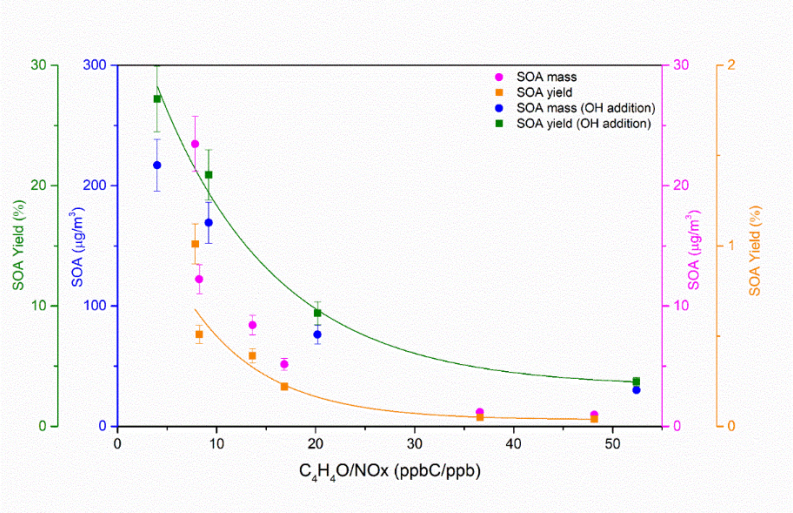

Figure 3: Dependence of the SOA mass concentration and SOA yield on the C_4H_4O/NOx ratio. Since the particle wall loss has a weak RH dependence in our chamber, a mean value of 3.6×10^{-5} s^{-1} was used for wall loss correction. A density of 1.4 g cm^{-3} was used in SMPS (Jia and Xu, 2018; Kostenidou et al., 2007).

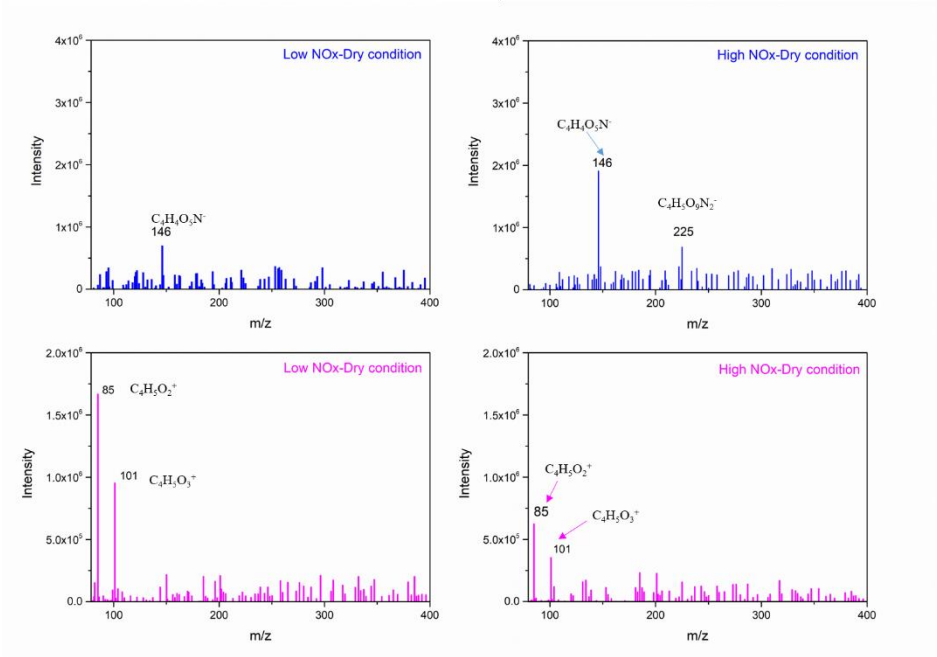

Figure 7: Selected background-subtraction HESI-Q Exactive-Orbitrap MS results of SOA in both negative (blue) and positive (pink) ion modes from the photooxidation of furan under different RH conditions.

Table S1. Summary of experimental conditions with the additional injection of H_2O_2 in the study of the NOx effect on SOA formaiton.

No.	$[furan]_0$ (ppb)	$[H_2O_2]_0$ (ppm)	$[NOx]_0$ (ppb)	RH (%)	C_4H_4O/NOx (ppbC/ppb)	SOA[e] ($\mu g\ m^{-3}$)	SOA yield (%)
13	802	1.7	15.3	< 10	52.4	30.1	3.7
14	811	1.6	40.2	< 10	20.2	76.3	9.4
15	807	1.7	87.5	< 10	9.2	169.2	20.9
16	797	1.7	200.1	< 10	4.0	216.9	27.2

Table S2. Summary of experimental conditions for HESI-Q Exactive-Orbitrap MS detection.

No.	$[furan]_0$ (ppb)	$[H_2O_2]_0$ (ppm)	$[NOx]_0$ (ppb)	RH (%)	C_4H_4O/NOx (ppbC/ppb)	Aim
17	723.5	3.5	26.4	<5	36.3	for HESI-Q Exactive-Orbitrap MS
18	748.3	6.5	152.6	<5	5.8	
19	764.8	7.2	163.5	30	5.9	
20	755.1	7.3	149.8	62	5.9	

RH dependence of SOA yields

Again, as H2O is used to generate OH radicals, higher RH levels result in more OH radicals, which lead to more SOA mass produced from furan photooxidation. **The**

observed 'RH effect' is essentially another 'OH effect' by promoting the generation of OH radicals and accelerating the oxidation processes of furan. The authors suggest that relative humidity affects the SOA yield through aqueous phase chemistry. However, the deliquescence point of sodium chloride is around 70% RH, below which the water content in the NaCl particles is close to zero, meaning that there would be minimal aqueous phase chemistry occurring in the particle phase.

Author reply:

The DRH and ERH of NaCl are about 75.5% and 47.6-46.3% (Gupta et al., 2015), respectively. NaCl seed aerosols were generated via atomization of NaCl aqueous solution with a constant-rate atomizer. The seed particles would be in the form of droplets after produced from the atomizer (Ge et al., 2016). Being dried through a self-made diffusion dryer, the NaCl seeds experienced efflorescence behavior during the dehydration process. It has been previously shown that SOA formation decreases both the ERH and DRH of the seed particles and results in the uptake of water by the particles (Liu et al., 2018; Takahama et al., 2007; Smith et al., 2012). There is a high possibility that the NaCl seeds will effloresce and deliquesce early after being coated by the new formed SOA. This assumption has been mentioned in the manuscript on Page 14, line 17. Additionally, we have monitored the aerosol liquid water content after the experiments. The details for the detection of ALW have been presented on Page 5, line 23 in our manuscript. Furthermore, as displayed in the manuscript, the ALW content has been indeed detected at 54% RH. Therefore, there is a high possibility that aqueous phase chemistry may play an important role in the SOA formation. This assumption was further confirmed by the results of HESI-Q Exactive-Orbitrap MS. The appearance of m/z^+ 185 and m/z^- 262 demonstrated that aqueous phase reactions indeed took place under high RH conditions by aqueous phase reaction of the hydroxyfuranone (B) and 1,4-dialdehyde (D) (Strollo and Ziemann, 2013). Alternatively, the moist surface under high RH conditions is more favorable for the condensation of the products with carbonyl functional groups,

leading to the increasing production of SOA formation. As shown in Fig. 8, the intensities of multifunctional hydroxyl nitrates and dihydroxyl dinitrate (m/z$^-$ 146, 225) exhibited positive correlations with RH conditions. Slight peak intensity increases of m/z+ 85 and 101 products were also observed under high RH conditions, indicating that the gas-particle phase partitioning of low-volatility compounds was enhanced at these conditions. The discussion concerning the effect of RH on furan SOA formation has been rewritten to provide more information.

Page 9, line 28:

"It is worth note that under high RH conditions, as shown in Fig. 1, the NO_2 hydrolysis (reaction (R11)) can generate nitrous acid (HONO), which has been considered as a major source of OH. As indicated in Fig. 4, the SOA yields obtained in the present work clearly show a gradual increase with RH. Also shown in Fig. S3 is the dependence of OH and furan concentrations on RH during the experiments determined from the decay of furan using a reaction rate coefficient of k(OH+furran) = 4.01×10^{-11} cm^3 $molecules^{-1}$ s^{-1} (Atkinson et al., 1983). It is therefore probable that the increase of RH results in high levels of HONO formation in the chamber, which leads to an increase in OH concentration, a faster furan decay rate, and higher aerosol mass yields. This result is in reasonable good agreement with previous studies, which proposed that the amount of products that can partition into the particle phase increases with the increasing rate of hydrocarbon oxidation (Healy et al., 2009; Chan et al., 2007). Moreover, the increasing RH might also enhance the SOA formation due to the fact that the functionalized gas phase components were more favoured to condense on the surface of wet particles (Liu et al., 2019b)."

Page 13, line 3:

"**3.4 Effect of RH on SOA formation**

Experiments 6-12 were conducted under seven different RH conditions ranging from 5% to 85%. In this RH range, the SOA yield increases from 1.01% to 5.03%.

With almost identical initial conditions except RH, the yield of furan-derived SOA formed at high RH can be a factor of two higher than that formed at low RH. A similar trend was also observed by Yu et al., who found that the SOA mass concentrations increased by a factor of six when RH increased from 18% to 82% (Yu et al., 2011). As shown in Fig. S3, an increase in RH leads to higher OH concentrations resulting from higher HONO levels generated by the reaction of NO_2 with H_2O. Previously, Anglada et al. confirmed, using quantum mechanical calculations, that the water component could increase the OH production (Anglada et al., 2011). The positive correlation between initial water vapour concentration and OH concentration has also been previously observed experimentally (Healy et al., 2009; Tillmann et al., 2010). Additionally, Healy et al. have also reported that increasing OH concentration promoted the decay of VOC and enhanced SOA formation (Healy et al., 2009). Similarly, in the present work, a faster decay rate of furan was also observed as RH increased, as shown in Fig. S3. It is possible that the faster rate of gas phase oxidation under higher OH concentrations will lead to the generation of less volatile compounds as presented previously (Chan et al., 2007). A higher OH concentration promotes oxidation reactions, influences the distribution of organic products, and facilitates the SOA formation (Sarrafzadeh et al., 2016b).

An obvious increase of SOA yield was observed when the RH increased from 37% to 54%. This phenomenon was mainly caused by the efflorescence transition when the seed particles were coated with SOA. It has been previously shown that SOA formation decreases both the efflorescence RH and deliquescence RH of the seed particles and results in the uptake of water by the particles (Liu et al., 2018; Takahama et al., 2007; Smith et al., 2012). It is highly possible that the NaCl seeds effloresce and deliquesce early after being coated by the new formed SOA. The effect of efflorescence contributes to the water uptake by the particles, leading to the obvious trend-changing of SOA yield. It is noted that with the NaCl seed aerosols serving as nuclei, the ALW was high at high RH. Products with water solubility produced from the photooxidation of furan can dissolve into the ALW of aerosol particles. As a result,

ALW in the formed aerosols plays an important role in gas/particle partitioning. As shown in Fig. 4, the ALW was detected when the RH was higher than 54%, which was based on the deliquescence of NaCl under high RH conditions. The increase of ALW could partially explain the increase of SOA mass concentration and SOA yield. It is highly probable that the particle surface area increases with increasing amount of ALW as shown in Fig. S7, which likely promotes the dissolution of semi-volatile matters produced during the experiments. According to the HESI-Q Exactive-Orbitrap MS results shown in Fig. 8, the intensities of multifunctional hydroxyl nitrates and dihydroxyl dinitrate (*m/z*$^-$ 146 and 225, respectively) exhibited positive correlations with RH. Slight peak intensities increases of m/z$^+$ 85 and 101 products were also observed under high RH conditions. This phenomenon indicates that the gas-particle phase partitioning of low-volatility compounds was enhanced under high RH conditions. Furthermore, the increased surface area under high RH conditions may also be attributed to the condensation of the produced multifunctional compounds.

Another possibility for the increasing trend of SOA yield with the increase of RH might result from the SOA formation through aqueous chemistry in wet aerosols (Grgic et al., 2010; Lim et al., 2010). In these atmospheric processes, alcohols, aldehydes, and ketones formed from the photooxidation of furan in the gas phase can be absorbed into the humid surface of the hygroscopic SOA at high RH. This process further contributes to the formation of low-volatility products on the SOA surface. In addition, the aqueous photochemistry of highly soluble small compounds that portioned in ALW could produce additional organic compounds and result in larger SOA yield under high RH conditions (Faust et al., 2017; Jia and Xu, 2014). The appearance of *m/z*$^+$ 185 and *m/z*$^-$ 262 detected by the HESI-Q Exactive-Orbitrap MS further demonstrated that aqueous phase reactions indeed took place under high RH conditions. As shown in Scheme 1, the peak of *m/z*$^+$ 185 could form by aqueous phase reaction of the hydroxyfuranone (B) and 1,4-dialdehyde (D). The formation of hemiacetal (E) has also been detected by a previous study of the OH-initiated reaction of 3-methylfuran in the presence of NOx (Strollo and Ziemann, 2013). The proposed

hemiacetal compound (E) plays a substantial role in the obvious increase of m/z^+ 185 product formation under high RH conditions. A pathway of organonitrate (m/z^- 262) formation in the aqueous particles with the presence of NO_3^- was suggested in the present study based on a previous work, which indicated a radical-radical reaction pathway for organosulfate formation from aqueous OH oxidation of glycolaldehyde in the presence of sulfuric acid (Perri et al., 2010). Increasing the RH also resulted in an overall addition of peak intensities in the negative ion mode, due to the fact that the sample obtained at high RH during the SOA generation had a larger particle surface. Specifically, a relatively stronger intense band of $C_8H_8O_9N^-$ (m/z^-=262) was found under a high RH. Consequently, the heterogeneous products in wet seed particles will further contribute to the formation of SOA, because higher aerosol liquid water content enables more aqueous phase reactions.

In conclusion, the reasons for the increasing trend of SOA formation under high RH conditions may be summarized as following: firstly, higher concentration of OH radical will certainly promote the SOA formation as RH increases. A faster decay rate of furan will also contribute to the formation of products that can partition into the particle phase. In addition, it is possible that the aqueous surface of seed particles provides a new substrate for the photooxidation of furan. Previously, N_2O_5 and HNO_3 have been proven to be the key products in the VOC-NOx irradiation experiments (Wang et al., 2016). The moist surface under high RH conditions is more favorable for the condensation of products with low vapor pressure, leading to the increasing production of SOA formation. The high RH environment favors the formation of the hemiacetal compound. Moreover, the effect of RH on SOA formation in furan photooxidation can also be determined by the aqueous photochemistry under high RH conditions as discussed above. The aqueous phase reactions at the surface of particles promotes the formation of hemiacetal-like products, which likely plays an important role in the process of SOA formation. Previously, unsaturated first-generation reaction product of 3-methyl furan has also been suggested to undergo acid-catalyzed condensed-phase reactions, with SOA yields up to 15% (Strollo and Ziemann, 2013).

In addition, the reinforced effect of RH on SOA yield was also ascribed from the photooxidation of other aromatic compounds, such as, benzene (Ng et al., 2007), toluene (Hildebrandt et al., 2009; Kamens et al., 2011), and xylene (Zhou et al., 2011)."

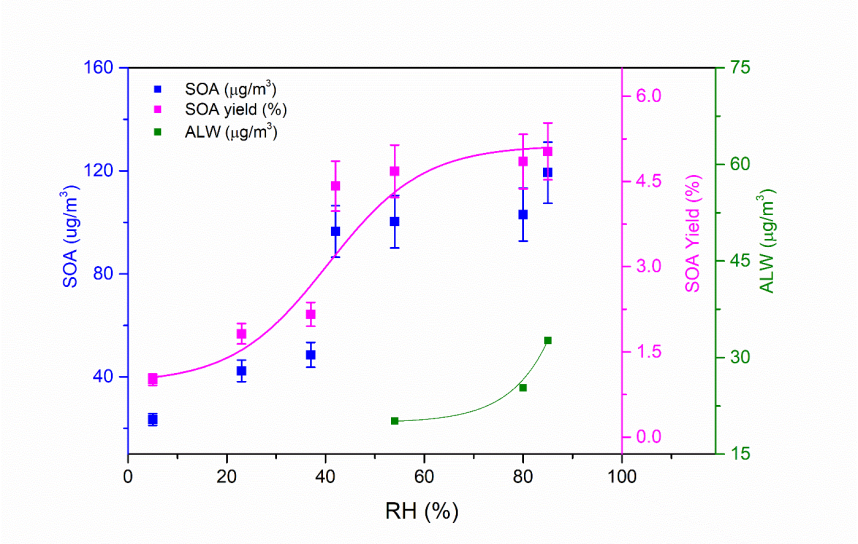

Figure 4: Dependences of the SOA mass concentration, SOA yield and ALW on relative humidity (RH).

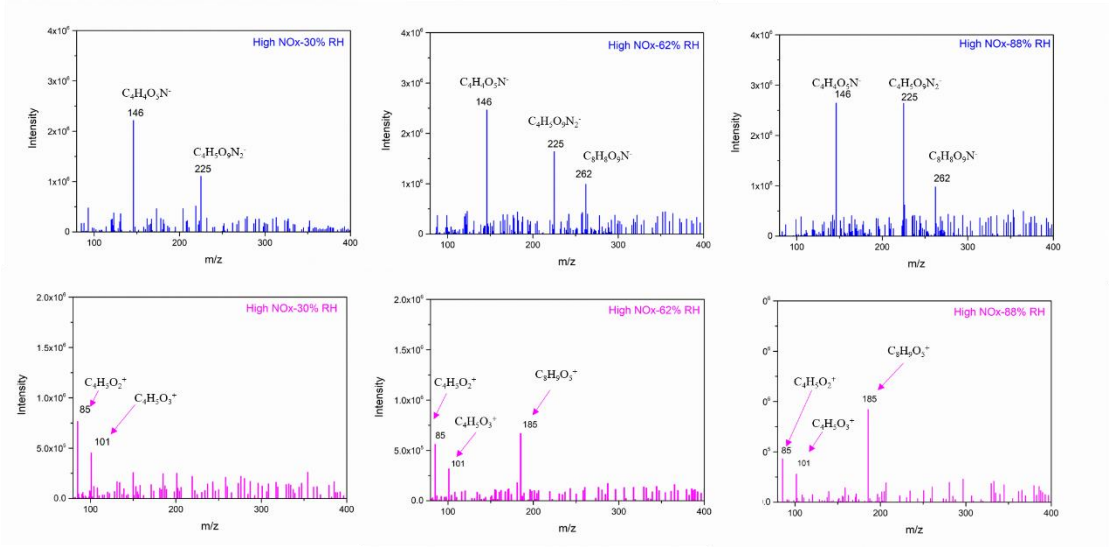

Figure 8: Selected background-subtraction HESI-Q Exactive-Orbitrap MS results of SOA in both negative (blue) and positive (pink) ion modes from the photooxidation of furan under different RH conditions.

SOA measurements at high RH levels

It is well known that using DMA to measure aerosol size distribution and mass leadings under high RH is subject to many certainties, e.g., arcing at high voltage caused by high water content in the aerosols. While the authors used a diffusion drier in front of the DMA inlet, which could certainly minimize the arcing effect that interferes the measurement of big particles, the drying efficiency was not characterized. Have the authors measured the RH of the aerosol flow upon the exit of the diffusion drier? Did aerosols generated under high RH (e.g., 80%) still carry a certain amount of water after drying? Additionally, the authors need to consider how the drying processes affect the repartitioning of water-soluble components between gas and particle phases in order to obtain an accurate SOA yield.

Author reply:

Indeed, the Nafion dryer was added to determine the liquid water content in the aerosols under high RH after the reaction ended. After modifying to the dry mode, the humid air in SMPS was quickly replaced by dry air through venting the sheath air at 5 L min^{-1}, and then the dry aerosol was measured by SMPS. The ALW was determined by the difference of the particle mass concentrations before and after the modification of the dry mode. After the dry mode treatment, the RH in the sampling air and sheath air reduced to 10 % and 7 %, respectively. The drying process for ALW determination is based on a widely used method developed by Engelhart (Engelhart et al., 2011), which has been proven to remove 90% of the water vapor. Consequently, the aerosols treated after the drying process were thought to carry seldom water content. We agree with the Referee that there is a possibility of the water-soluble components repartitioning betweent gas and particle phases. The fact that the SOA concentration for high RH conditions were slightly underestimated due to the ALW measurement. Thus, we added some sentences to reply comment on how the ALW meaurement affects our results on Page 5 in the revised manuscript.

"It should be noted that the dissloved water-soluble species would evaporate back into

the gas phase during the ALW measurement when the aerosol water is removed. In fact, the repartitioning of water-soluble components between gas and particle phases was not taken into consideration. The SOA concentrations for high RH conditions were slightly underestimated, but the underestimation is extremely low and can be negligible."

Treatment of wall losses

The particle and vapor wall loss rates are chamber specific quantities that depend on a number of different parameters, i.e., the chamber size (volume to surface area ratio), the wall materials, the humidity in the enclosure air that affects the static charges on the chamber wall surface, and the mixing conditions (static or active mixing), among many others. The interaction patterns of particles with the chamber walls have been well studied for decades, and the particle wall loss rate has been found to vary substantially, by orders of magnitude, among different chamber environments. That the authors simply took the particle wall loss parameterizations obtained in other chambers to correct their own experiment would no doubt introduce significant uncertainties in their SOA mass measurements, resulting in unreliable SOA yield calculations.

Author reply:

We agree with the Referee that the wall loss rates of different chambers are different and the difference is dependent on many parameters, such as, the chamber size, the wall materials, and the chamber environments. The particle and vapor wall loss parameterizations used in this study are based on a previous study carried out in the same chamber reactor in our lab. Besides the chamber size and wall material, the experimental environments of these two studies are also similar: i) both studies were conducted in the ~5%-80% humidity range; ii) in both studies, NaCl seeds were added at the beginning of each experiment to provide sufficient seed surface area to limit the effects of vapor wall losses; iii) during all experiments in these two studies, two

ironing air blowers were around the reactor to get rid of the electric charge on the surface of the reactor. Consequently, the citation of wall loss parameterizations detected from the same chamber reactor and similar experimental experiments will not introduce much uncertainties in the present study. After careful analysis of our experiments, we believe that our results are reliable and credible. To clarify the statement, we modified the sentences in the revised manuscript. The new one reads as follows:

"The wall loss rate constants for O_3, NOx and aerosol particles were 3.3×10^{-7} s^{-1}, 4.1×10^{-7} s^{-1}, and 3.6×10^{-5} s^{-1}, respectively, which were detected from our previous study conducted in the same set-up and similar experimental conditions (Ge et al., 2017a)."

References

Anglada, J. M., Gonzalez, J., and Torrent-Sucarrat, M.: Effects of the substituents on the reactivity of carbonyl oxides. A theoretical study on the reaction of substituted carbonyl oxides with water, Phys. Chem. Chem. Phys., 13, 13034-13045, 10.1039/c1cp20872a, 2011.

Aschmann, S. M., Nishino, N., Arey, J., and Atkinson, R.: Products of the OH radical initiated reactions of furan, 2-and 3-methylfuran, and 2,3-and 2,5-dimethylfuran in the presence of NO, J. Phys. Chem. A, 118, 457-466, 10.1021/jp410345k, 2014.

Atkinson, R., Aschmann, S. M., and Carter, W. P.: Kinetics of the reactions of O_3 and OH radicals with furan and thiophene at 298±2 K, Int. J. Chem. Kinet., 15, 51-61, 0.1002/kin.550150106, 1983.

Chan, A. W. H., Kroll, J. H., Ng, N. L., and Seinfeld, J. H.: Kinetic modeling of secondary organic aerosol formation: Effects of particle- and gas-phase reactions of semivolatile products, Atmos. Chem. Phys., 7, 4135-4147, 10.5194/acp-7-4135-2007, 2007.

Chan, A. W. H., Chan, M. N., Surratt, J. D., Chhabra, P. S., Loza, C. L., Crounse, J. D., Yee, L. D., Flagan, R. C., Wennberg, P. O., and Seinfeld, J. H.: Role of aldehyde chemistry and NOx concentrations in secondary organic aerosol formation, Atmos. Chem. Phys., 10, 7169-7188, 10.5194/acp-10-7169-2010, 2010.

Engelhart, G. J., Hildebrandt, L., Kostenidou, E., Mihalopoulos, N., Donahue, N. M., and Pandis, S. N.: Water content of aged aerosol, Atmos. Chem. Phys., 11, 911-920, 10.5194/acp-11-911-2011, 2011.

Faust, J. A., Wong, J. P. S., Lee, A. K. Y., and Abbatt, J. P. D.: Role of aerosol liquid water in secondary organic aerosol formation from volatile organic compounds, Environ. Sci. Technol., 51, 1405-1413, 10.1021/acs.est.6b04700, 2017.

Ge, S., Xu, Y., and Jia, L.: Secondary organic aerosol formation from propylene irradiations in a chamber study, Atmos. Environ., 157, 146-155, 10.1016/j.atmosenv.2017.03.019, 2017.

Grgic, I., Nieto-Gligorovski, L. I., Net, S., Temime-Roussel, B., Gligorovski, S., and Wortham, H.: Light induced multiphase chemistry of gas-phase ozone on aqueous pyruvic and oxalic acids, Phys. Chem. Chem. Phys., 12, 698-707, 10.1039/b914377g, 2010.

Gupta, D., Kim, H., Park, G., Li, X., Eom, H. J., and Ro, C. U.: Hygroscopic properties of NaCl and NaNO3 mixture particles as reacted inorganic sea-salt aerosol surrogates, Atmos. Chem. Phys., 15, 3379-3393, 10.5194/acp-15-3379-2015, 2015.

Healy, R. M., Temime, B., Kuprovskyte, K., and Wenger, J. C.: Effect of relative humidity on gas/particle partitioning and aerosol mass yield in the photooxidation of p-Xylene, Environ. Sci. Technol., 43, 1884-1889, 10.1021/es802404z, 2009.

Hildebrandt, L., Donahue, N. M., and Pandis, S. N.: High formation of secondary organic aerosol from the photo-oxidation of toluene, Atmos. Chem. Phys., 9, 2973-2986, 10.5194/acp-9-2973-2009, 2009.

Hoyle, C. R., Boy, M., Donahue, N. M., Fry, J. L., Glasius, M., Guenther, A., Hallar, A. G., Hartz, K. H., Petters, M. D., Petaja, T., Rosenoern, T., and Sullivan, A. P.: A review

of the anthropogenic influence on biogenic secondary organic aerosol, Atmos. Chem. Phys., 11, 321-343, 10.5194/acp-11-321-2011, 2011.

Jia, L., and Xu, Y.: Effects of relative humidity on ozone and secondary organic aerosol formation from the photooxidation of benzene and ethylbenzene, Aerosol Sci. Tech., 48, 1-12, 10.1080/02786826.2013.847269, 2014.

Jia, L., and Xu, Y.: Different roles of water in secondary organic aerosol formation from toluene and isoprene, Atmos. Chem. Phys., 18, 8137-8154, 10.5194/acp-18-8137-2018, 2018.

Kamens, R. M., Zhang, H., Chen, E. H., Zhou, Y., Parikh, H. M., Wilson, R. L., Galloway, K. E., and Rosen, E. P.: Secondary organic aerosol formation from toluene in an atmospheric hydrocarbon mixture: Water and particle seed effects, Atmos. Environ., 45, 2324-2334, 10.1016/j.atmosenv.2010.11.007, 2011.

Kostenidou, E., Pathak, R. K., and Pandis, S. N.: An algorithm for the calculation of secondary organic aerosol density combining AMS and SMPS data, Aerosol Sci. Tech., 41, 1002-1010, 10.1080/02786820701666270, 2007.

Kroll, J. H., and Seinfeld, J. H.: Chemistry of secondary organic aerosol: Formation and evolution of low-volatility organics in the atmosphere, Atmos. Environ., 42, 3593-3624, 10.1016/j.atmosenv.2008.01.003, 2008.

Lim, Y. B., Tan, Y., Perri, M. J., Seitzinger, S. P., and Turpin, B. J.: Aqueous chemistry and its role in secondary organic aerosol (SOA) formation, Atmos. Chem. Phys., 10, 10521-10539, 10.5194/acp-10-10521-2010, 2010.

Liu, C., Liu, J., Liu, Y., Chen, T., and He, H.: Secondary organic aerosol formation from the OH-initiated oxidation of guaiacol under different experimental conditions, Atmos. Environ., 207, 30-37, 10.1016/j.atmosenv.2019.03.021, 2019a.

Liu, S., Tsona, N. T., Zhang, Q., Jia, L., Xu, Y., and Du, L.: Influence of relative humidity on cyclohexene SOA formation from OH photooxidation, Chemosphere, 231, 478-486, 10.1016/j.chemosphere.2019.05.131, 2019b.

Liu, T., Huang, D. D., Li, Z., Liu, Q., Chan, M., and Chan, C. K.: Comparison of secondary organic aerosol formation from toluene on initially wet and dry ammonium

sulfate particles at moderate relative humidity, Atmos. Chem. Phys., 18, 5677-5689, 10.5194/acp-18-5677-2018, 2018.

Loza, C. L., Craven, J. S., Yee, L. D., Coggon, M. M., Schwantes, R. H., Shiraiwa, M., Zhang, X., Schilling, K. A., Ng, N. L., Canagaratna, M. R., Ziemann, P. J., Flagan, R. C., and Seinfeld, J. H.: Secondary organic aerosol yields of 12-carbon alkanes, Atmos. Chem. Phys., 14, 1423-1439, 10.5194/acp-14-1423-2014, 2014.

Ng, N. L., Kroll, J. H., Chan, A. W. H., Chhabra, P. S., Flagan, R. C., and Seinfeld, J. H.: Secondary organic aerosol formation from m-xylene, toluene, and benzene, Atmos. Chem. Phys., 7, 3909-3922, 10.5194/acp-7-3909-2007, 2007.

Perri, M. J., Lim, Y. B., Seitzinger, S. P., and Turpin, B. J.: Organosulfates from glycolaldehyde in aqueous aerosols and clouds: Laboratory studies, Atmos. Environ., 44, 2658-2664, 10.1016/j.atmosenv.2010.03.031, 2010.

Sarrafzadeh, M., Wildt, J., Pullinen, I., Springer, M., Kleist, E., Tillmann, R., Schmitt, S. H., Wu, C., Mentel, T. F., and Zhao, D.: Impact of NOx and OH on secondary organic aerosol formation from β-pinene photooxidation, Atmos. Chem. Phys., 16, 11237-11248, 10.5194/acp-16-11237-2016, 2016a.

Sarrafzadeh, M., Wildt, J., Pullinen, I., Springer, M., Kleist, E., Tillmann, R., Schmitt, S. H., Wu, C., Mentel, T. F., Zhao, D., Hastie, D. R., and Kiendler-Scharr, A.: Impact of NOx and OH on secondary organic aerosol formation from beta-pinene photooxidation, Atmos. Chem. Phys., 16, 11237-11248, 10.5194/acp-16-11237-2016, 2016b.

Schwantes, R. H., Charan, S. M., Bates, K. H., Huang, Y., Nguyen, T. B., Mai, H., Kong, W., Flagan, R. C., and Seinfeld, J. H.: Low-volatility compounds contribute significantly to isoprene secondary organic aerosol (SOA) under high-NOx conditions, Atmos. Chem. Phys., 19, 7255-7278, 10.5194/acp-19-7255-2019, 2019.

Smith, M. L., Bertram, A. K., and Martin, S. T.: Deliquescence, efflorescence, and phase miscibility of mixed particles of ammonium sulfate and isoprene-derived secondary organic material, Atmos. Chem. Phys., 12, 9613-9628, 10.5194/acp-12-9613-2012, 2012.

Song, C., Na, K. S., and Cocker, D. R.: Impact of the hydrocarbon to NOx ratio on secondary organic aerosol formation, Environ. Sci. Technol., 39, 3143-3149, 10.1021/es0493244, 2005.

Strollo, C. M., and Ziemann, P. J.: Products and mechanism of secondary organic aerosol formation from the reaction of 3-methylfuran with OH radicals in the presence of NOx, Atmos. Environ., 77, 534-543, 10.1016/j.atmosenv.2013.05.033, 2013.

Takahama, S., Pathak, R. K., and Pandis, S. N.: Efflorescence transitions of ammonium sulfate particles coated with secondary organic aerosol, Environ. Sci. Technol., 41, 2289-2295, 10.1021/es0619915, 2007.

Tillmann, R., Hallquist, M., Jonsson, A. M., Kiendler-Scharr, A., Saathoff, H., Iinuma, Y., and Mentel, T. F.: Influence of relative humidity and temperature on the production of pinonaldehyde and OH radicals from the ozonolysis of alpha-pinene, Atmos. Chem. Phys., 10, 7057-7072, 10.5194/acp-10-7057-2010, 2010.

Wang, Y., Luo, H., Jia, L., and Ge, S.: Effect of particle water on ozone and secondary organic aerosol formation from benzene-NO_2-NaCl irradiations, Atmos. Environ., 140, 386-394, 10.1016/j.atmosenv.2016.06.022, 2016.

Yu, K.-P., Lin, C.-C., Yang, S.-C., and Zhao, P.: Enhancement effect of relative humidity on the formation and regional respiratory deposition of secondary organic aerosol, J. Hazard. Mater., 191, 94-102, 10.1016/j.jhazmat.2011.04.042, 2011.

Zhou, Y., Zhang, H., Parikh, H. M., Chen, E. H., Rattanavaraha, W., Rosen, E. P., Wang, W., and Kamens, R. M.: Secondary organic aerosol formation from xylenes and mixtures of toluene and xylenes in an atmospheric urban hydrocarbon mixture: Water and particle seed effects (II), Atmos. Environ., 45, 3882-3890, 10.1016/j.atmosenv.2010.12.048, 2011.